Available online at www.sciencedirect.com

SCIENCE DIRECT®

Journal of the European Ceramic Society 23 (2003) 2005–2014

www.elsevier.com/locate/jeurceramsoc

Synthesis of Si_3N_4 by the carbo-thermal reduction and nitridation of diatomite

Halil Arik

Department of Metallurgy, Faculty of Technical Education, Gazi University, Ankara 06500, Turkey

Received 28 July 2002; received in revised form 3 January 2003; accepted 13 January 2003

Abstract

A study was undertaken to production of Si_3N_4 powders by carbo-thermal reduction and nitridation (CTRN) of diatomite. Test samples were prepared by mixing 99% purity and mean powder size of 2.4 μm of carbon black and maximum particle size of 150 μm diatomite with C/SiO_2 molar ratio 4. Prepared sample was subjected to CTRN process at temperatures of 1300, 1350, 1400, and 1450 °C for 4, 8, and 16 h. CTRN process was conducted in an atmosphere controlled tube furnace in nitrogen flow 5 cm^3/min. All products were examined by XRD and SEM-EDX to determine the transformation, morphology and chemical composition. The results showed that the best Si_3N_4 transformation occurred at 1400 °C for 16 h.

Keywords: Carbothermal reduction; Diatomite; Nitridation; Si_3N_4

1. Introduction

Silicon nitride (Si_3N_4) is an attractive structural ceramic owing to its high temperature strength, toughness, wear resistance and thermal stability due to the low coefficient of thermal expansion. Because of these properties silicon nitride is the most promising material especially for high temperature engineering applications.[1–3] A variety of methods and techniques have been employed by various investigators to produce silicon nitride powders from raw materials as silicon source.[4–11] The well-known techniques are direct reaction between silicon (Si) and nitrogen (N_2), and carbothermal reduction of silica (SiO_2) with a source of carbon and at the same time, nitridation of it with nitrogen gas.[1,12,13]

Nitridation of metallic silicon powder:

$$3Si_{(s)} + 2N_{2(g)} \overset{1200\text{–}1500^\circ C}{\rightarrow} Si_3N_{4(s)} \tag{1}$$

Carbo-thermal reduction of SiO_2 in nitrogen atmosphere:

$$3SiO_{2(s)} + 6C_{(s)} + 2N_{2(g)} \overset{1200\text{–}1700^\circ C}{\rightarrow} Si_3N_{4(s)} + 6CO_{(g)} \tag{2}$$

To produce silicon nitride powders different raw materials (volcanic ash, kaolinite, illite, sepiolite, and zeolite) as a silicon source have been used by various investigators.[14–17] In this study diatomite as silicon source has been used.

Diatomite is a siliceous, sedimentary rock consisting principally of the fossilized skeletal remains of diatom, a unicellular aquatic plant related to the algae. The terms diatomaceous earth and kieselguhr are used synonymous with diatomite. The silica of fossilized diatom skeleton closely resembles opal or hydrous silica in composition ($SiO_2.nH_2O$). In addition to bound water, varying between 3.5 and 8%, the siliceous skeleton may also contain, in solid solution, or as part of the SiO_2 complex, small amounts of associated in organic components—alumina, principally—and lesser amounts of iron, alkaline earth, alkali metals, and other minor constituents. Processed diatomite possesses an unusual particulate structure and chemical stability that lends itself to applications not filled by any other form of silica. Foremost among these applications is its use as a filter aid, which accounts for over half of its current consumption. Its unique diatom structure, low bulk density, high absorptive capacity, high surface area, and relatively low abrasion are attributes responsible for its utility as a functional filler and as an extender in paint,

---

E-mail address: harik@gazi.edu.tr (H. Arik).

doi:10.1016/S0955-2219(03)00038-4

paper, rubber, an in plastics; and thermal insulating material; polish, abrasive to name a few representative applications.[18–20]

2. Experimental procedure

2.1. Material

The diatomite, used throughout the investigation as source of silica, was obtained from the Kızılcahamam area of Turkey. Chemical composition of as-received diatomite is given in Table 1. Initially, XRD, DTA and SEM-EDX analyses were performed on the diatomite samples. XRD analysis indicated that diatomite had a completely amorphe structure and DTA–TG curves showed that until 320 °C diatomite had lost 2.8% of its weight which are related to the release of surface water and the zeolitic water of diatomite (Fig. 1). SEM micrograph showed that the porously morphology of as-received diatomite (Fig. 2). Carbon black with 99% purity was used as the source of carbon, and its specifications are given in Table 2. The nitrogen gas used contained less than 5 ppm O_2 and H_2O.

2.2. Effect of the heating on behavior of diatomite

Sapless of diatomite were heated for 4 h in a furnace open to atmosphere at temperatures of 500, 800, 900, 1000, 1100, 1200, 1300, 1400, and 1450 °C. The heating rate to the desired temperature was approximately 5 °C min^{-1}. The furnace was held at the desired temperature with accuracy of ± 5 °C, and then cooled at 5 °C min^{-1} to room temperature. Then all of the products were analysed by XRD and SEM EDX to determine the structural transformation taking place during the heating.

2.2.1. XRD and SEM analysis

XRD analysis of the products heated up to 800 °C showed no formation of phase other than those belonging to amorph structure of diatomite. The product maintained the porously morphology of diatomite. Firstly at 900 °C, peak of diatomite slightly disappeared while the peaks of cristobalite and quartz appeared. At 1100 °C, peaks of quartz totally disappeared and all of the characteristic peaks of cristobalite appeared. At 1200 °C the intensity of cristobalite peaks increased relative to the peak intensity at 1100 °C. Oxides of Al_2O_3, Fe_2O_3, CaO, MgO, TiO_2, Na_2O, and K_2O in the diatomite-structure formed liquid phase due to eutectic reactions at 1200 °C, and the porously morphology of diatomite agglomerated (Fig. 3). At 1300–1450 °C, cristobalite phase was maintained with some increase in peak intensities corresponding to more crystallization (Fig. 4).

Table 1
Chemical analysis of the diatomite (wt.%)

SiO_2	Al_2O_3	Fe_2O_3	CaO	MgO	Na_2O_3	K_2O	TiO_2	P_2O_5	Loss of ignition
88.32	3.47	0.48	0.42	0.26	0.17	0.28	0.18	0.10	5.84

2.3. Carbo-thermal reduction and nitridation (CTRN) of diatomite

Diatomite was thoroughly mixed with carbon black in C/SiO_2 molar ratio of 4. Mixing was performed in a mill with alumina balls for 10 h. Then four-gram sample of the mixture was put in graphite boat having dimensions 15 mm×30 mm×60 mm. Then the boat was placed in an atmosphere-controlled tube furnace (Fig. 5) and then heated to test temperature in nitrogen (N_2) flow of 5 cm^3/min, and maintained for predetermined time. Under the identical test conditions, CTRN process for four mixtures was performed at 1300, 1350, 1400, and 1450 °C for 4, 8, and 16 h. Carbonitriding reaction was followed by the weight loss, the weight change was determined by weighing the samples before and after the reaction process. Residual carbon after reaction was determined through a loss on ignition (air) at 800 °C for 2 h. Then all products obtained at different temperatures and times by CTRN process were characterized by using X-ray Diffraction with Cu K_α radiation at 40 kV and 30 mA, Scanning Electron Microscopy (SEM), and Energy Dispersif X-ray (EDAX) (Jeol JSM 6400-Noran Instrument Series II). The ratio of α/β Si_3N_4 was estimated from XRD peak heights.

3. Results and discussion

3.1. Temperature

From XRD results it was seen that, carbo-thermal reduction and nitridation did not take place at 1300 °C. XRD and SEM-EDX analysis results were similar to the ones belonging to the fired diatomite at the same temperature. This result means that no reaction of SiO_2 took place at this temperature. It is common believe that SiO_2 will not be reduced at this temperature.[13,16] First transformation peaks were recorded in CTRN processing at 1350 °C. These peaks were partly belonging to α-Si_3N_4, β-Si_3N_4, and cristobalite peaks (Fig. 6). Temperature is still not sufficient for complete reduction of SiO_2[13,16,21] so partial reduction and nitridation took place.

Major reduction of SiO_2 took place at 1400 °C. The transformation products showed very strong Si_3N_4 peaks for all CTRN process times (Fig. 7). Increasing CTRN temperature to 1450 °C did not produced any further increase in reduction and nitridation. This is explained by partial melting of diatomite at this temperature. Thus

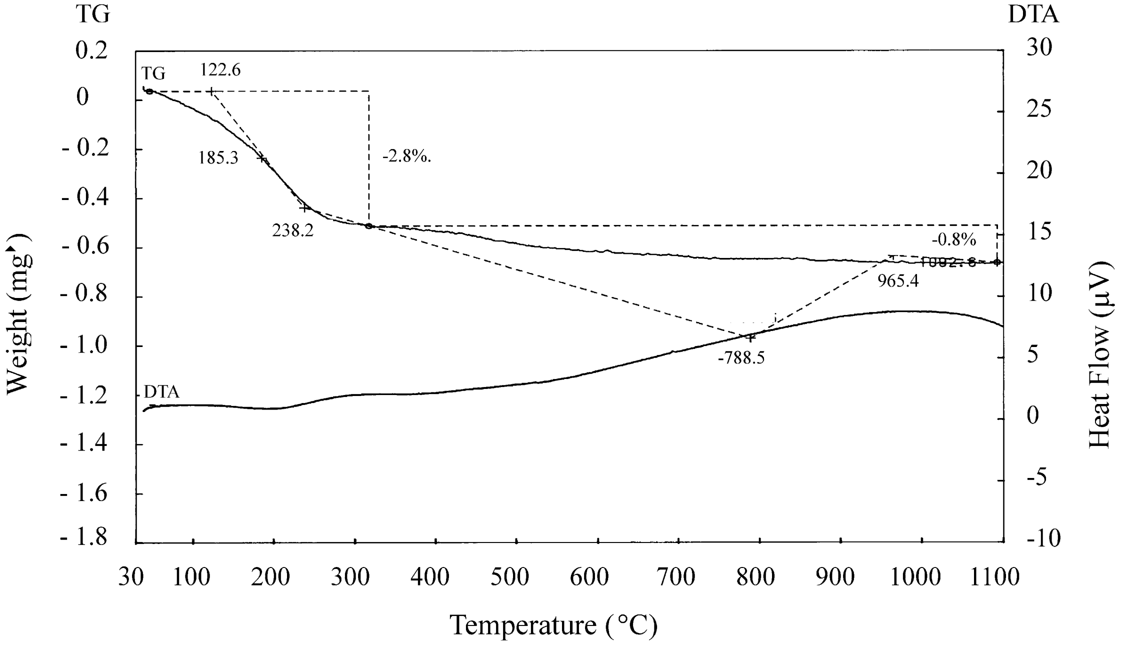

Fig. 1. DTA–TG curves of diatomite.

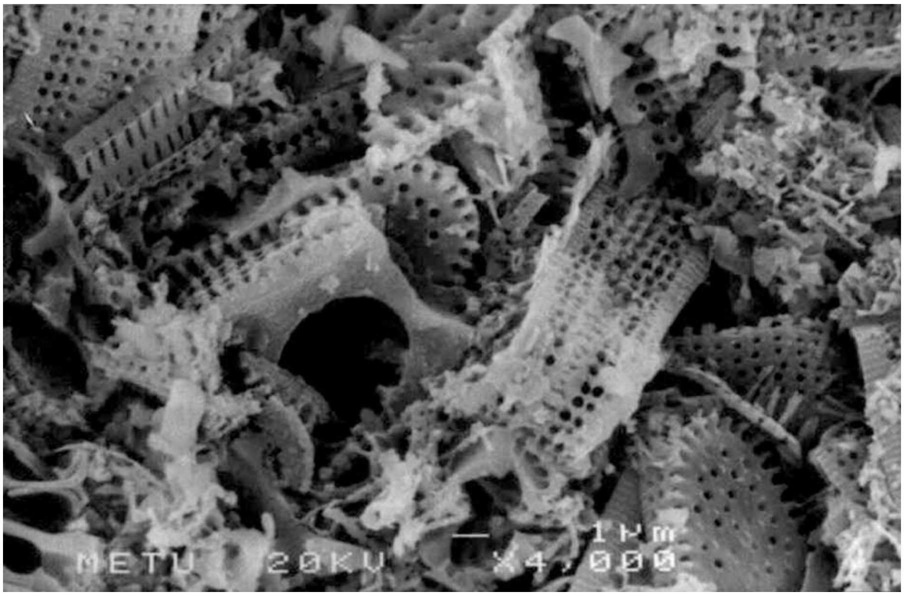

Fig. 2. SEM micrograph of diatomite.

Table 2
Specifications of carbon black

Reflection (%, with toluene)	325 mesh—sieve oversize (%)	Moisture (%)	Density (g/l)	Sulfur (%)
Min. 80	Min. –	Min. –	Min. 320	Min. –
Max. –	Max. 0.1	Max. 2.5	Max. 380	Max. 1

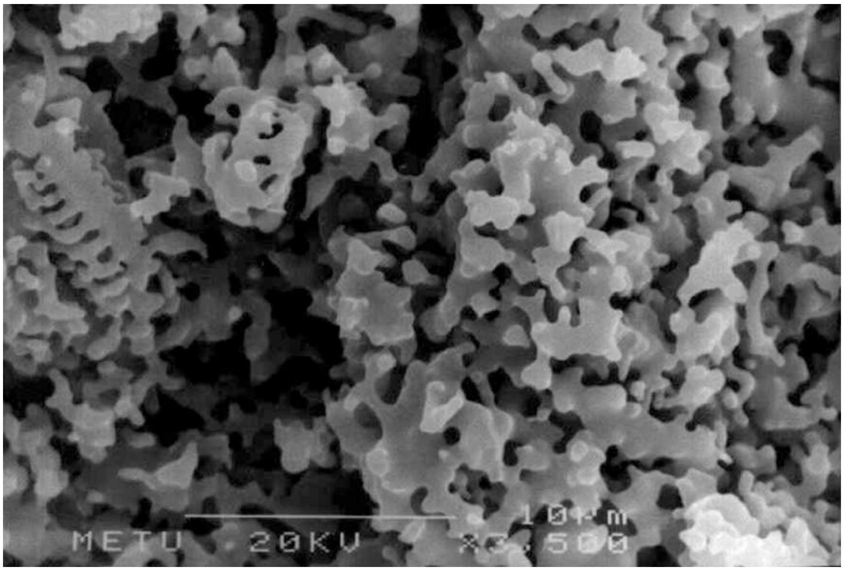

Fig. 3. SEM micrograph of diatomite heated at 1200 °C for 4 h.

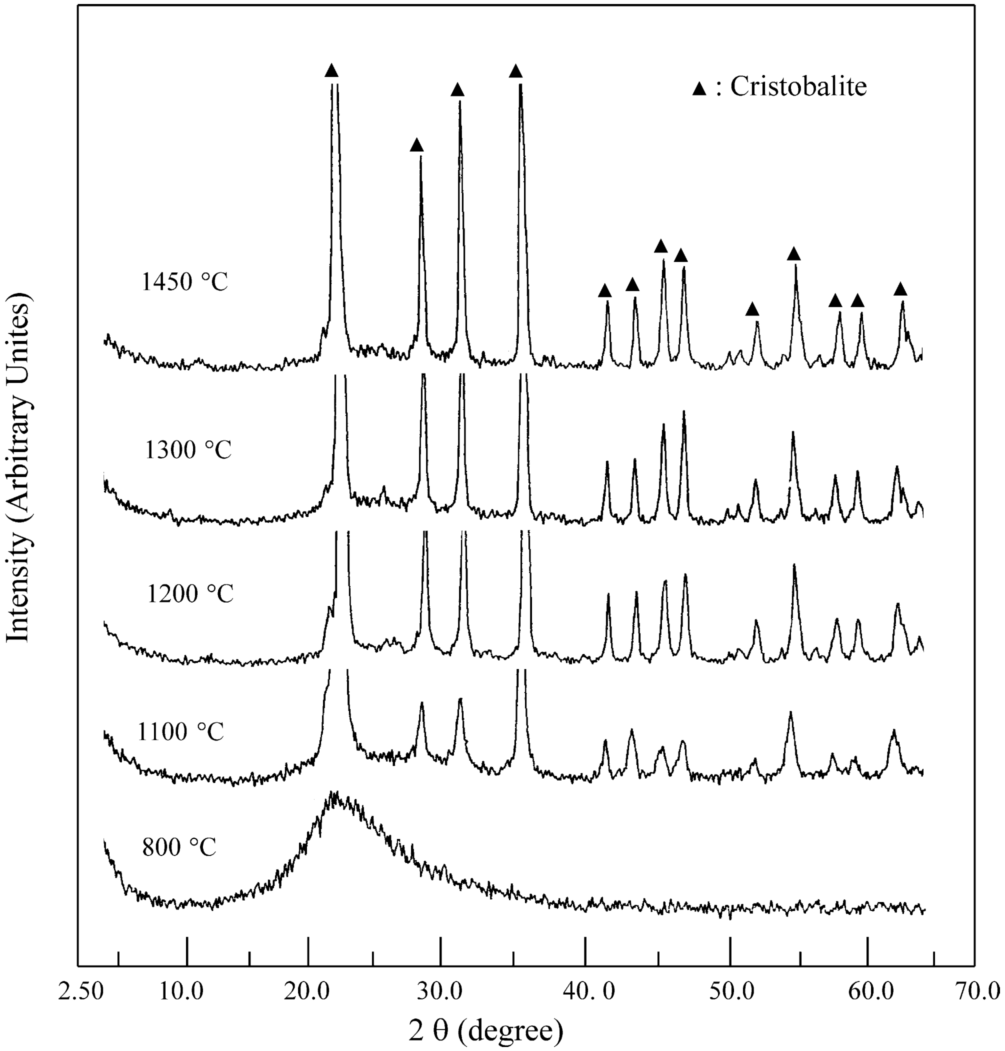

Fig. 4. XRD patterns of diatomite heated for 4 h at various temperatures (800–1450 °C).

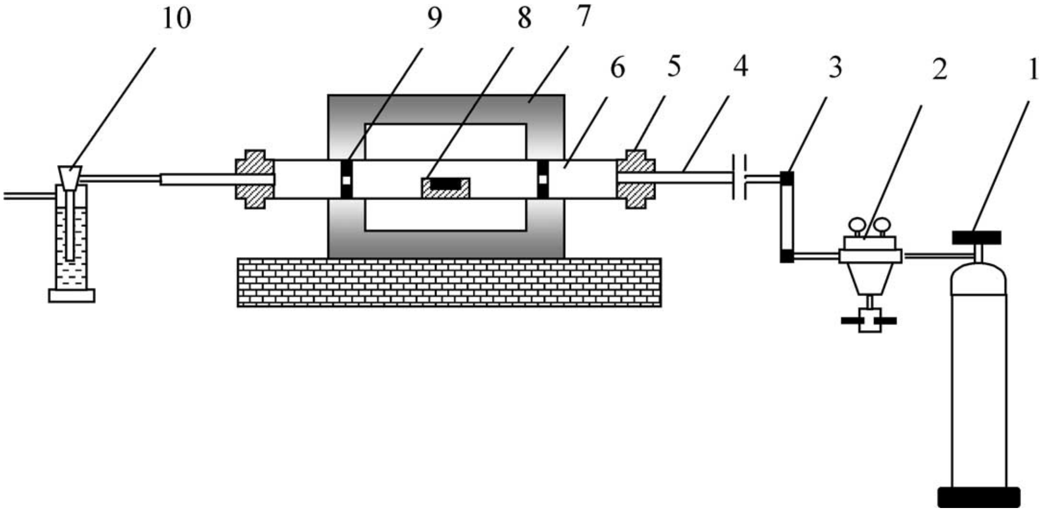

Fig. 5. Carbo-thermal reduction and nitridation set-up: 1 = nitrogen cylinder, 2 = pressure regulator, 3 = rotameter, 4 = plastic hose, 5 = graphite end connector, 6 = alumina furnace tube, 7 = furnace, 8 = sample boats, 9 = anti-radiation block, 10 = dissociation bottle.

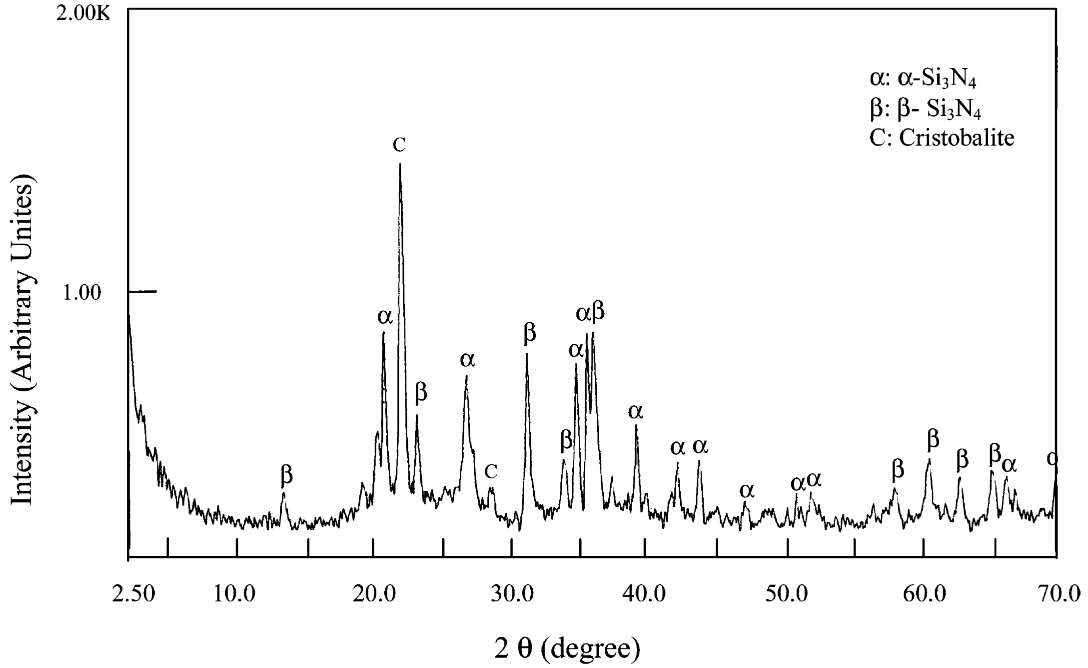

Fig. 6. XRD pattern of CTRN product obtained at 1350 °C for 16 h.

micro-porous structure harmed and surface area dramatically reduced with the presence of liquid phase which will decrease the transport of reaction gases. At 1450 °C, similar results were obtained for all treatment times but the XRD peaks were weaker (Figs. 8 and 9).

After 4 and 8 h CTRN treatment at 1400 and 1450 °C cotton-like structure was formed on the top of the boat and also on the walls of the tube furnace. XRD results showed that this cotton-like product consist of α-Si_3N_4, β-Si_3N_4, and SiC phases. 1450 °C is accepted as critical temperature in the literature for CTRN process.[16] At this temperature SiC may form instead of Si_3N_4. In this study, XRD analysis of the products obtained at 1400 and 1450 °C for 4 and 8 h CTRN process showed that approximately 5–10 wt.% of resulting products was belonging to silicon carbide phase (Fig. 10).

From the stoichiometry of the carbonitriding reactions it is clearly deduced that there is a direct relation between the consumed carbon (residual carbon) and the weight loss of the samples. If only carbonitriding reactions occurred it would be easy to calculate the residual carbon according to the weight loss. However, in the "Diatomite–C–N_2" reactions the removal of $SiO_{(g)}$ always occurred. In this case, reactions (4) and (5) takes

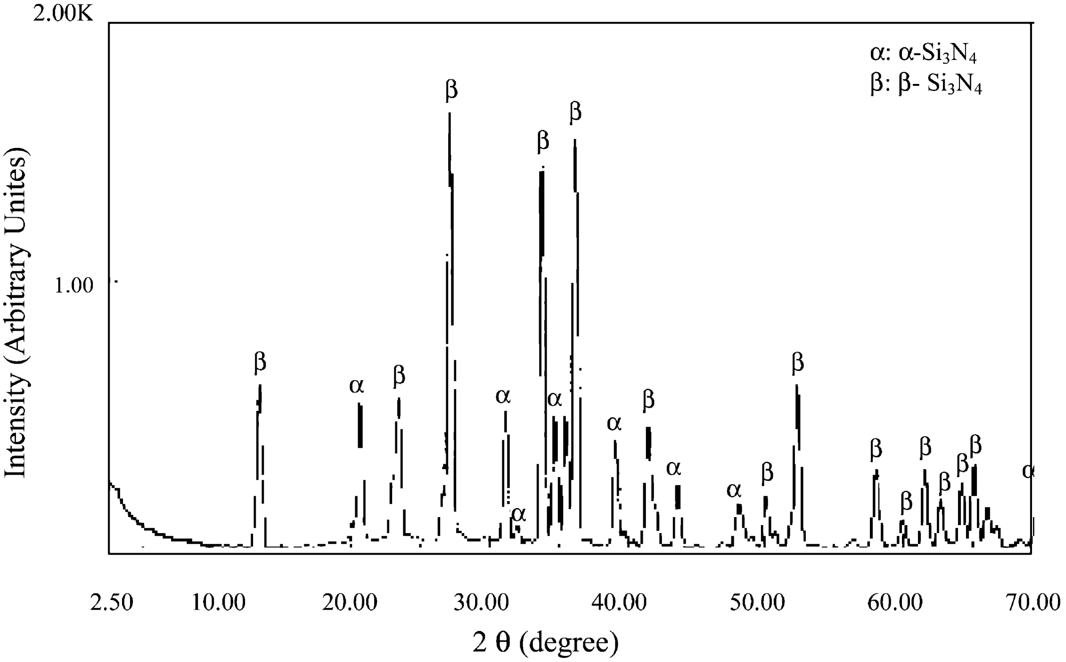

Fig. 7. XRD pattern of CTRN product obtained at 1400 °C for 16 h.

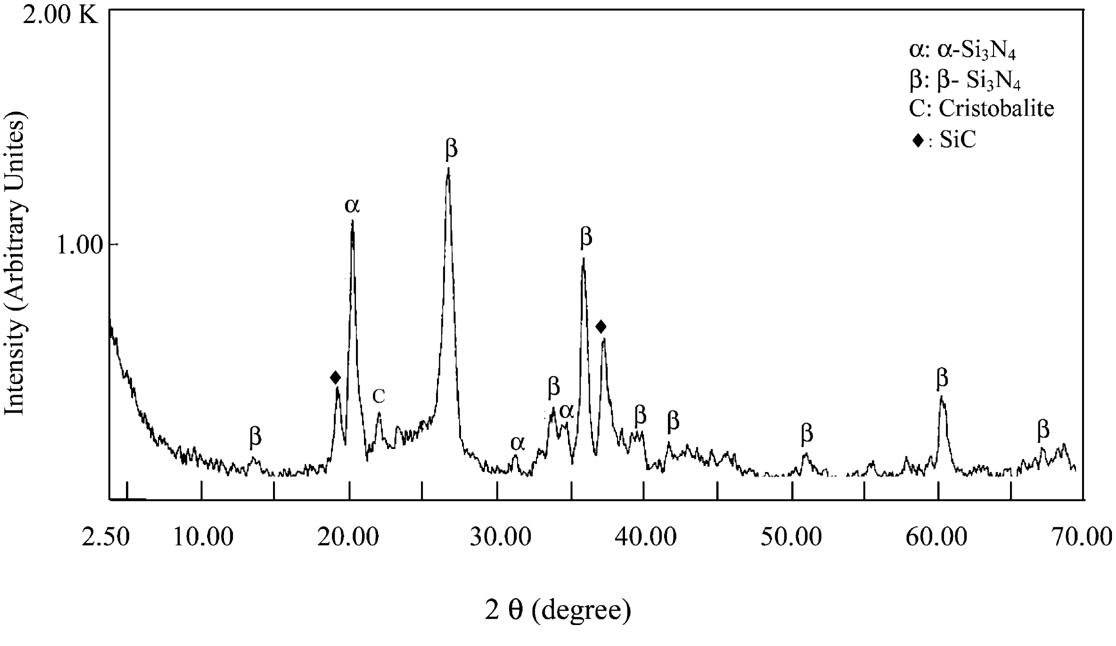

Fig. 8. XRD pattern of CTRN product obtained at 1450 °C for 4 h.

place. These reactions cause a higher weight loss per carbon gram consumed than the carbonitriding reaction and consequently the residual carbon content of samples is higher than the theoretical one expected by carbonitriding. In Table 3 some values of residual carbon determined by calcination in air and the theoretical residual carbon contents (wt.%) are shown. Table 3 shows that with increasing the CTRN temperature and duration the amount of the reduction and nitridation of diatomite is also increasing.

SEM analysis showed that resulting products obtained at 1400 and 1450 °C for 4 and 8 h CTRN process basically have two different morphology as fibrous and hexagonal prisms. While fibrous transformation structure is covering the top of the graphite boats, hexagonal prisms were located at the bottom of the boats (Fig. 11). The products obtained at 1400, and 1450 °C for 16 h CTRN process have predominantly hexagonal Si_3N_4 particles formed at the bottom of the graphite boats. Hexagonal Si_3N_4 particles have

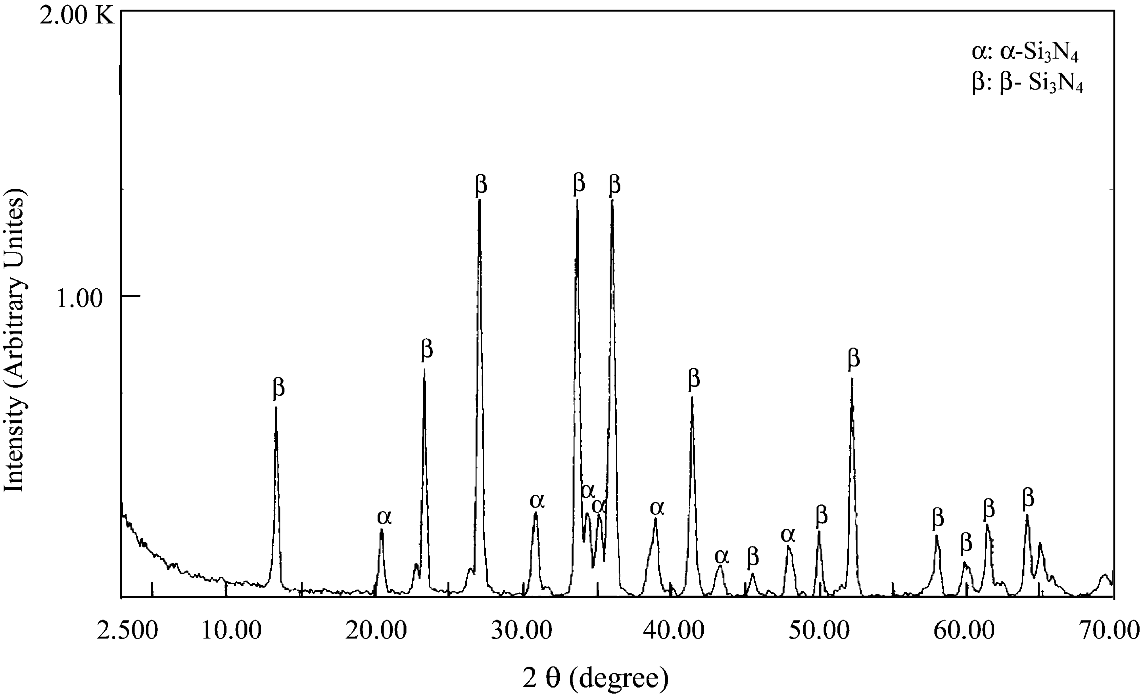

Fig. 9. XRD pattern of CTRN product obtained at 1450 °C for 16 h.

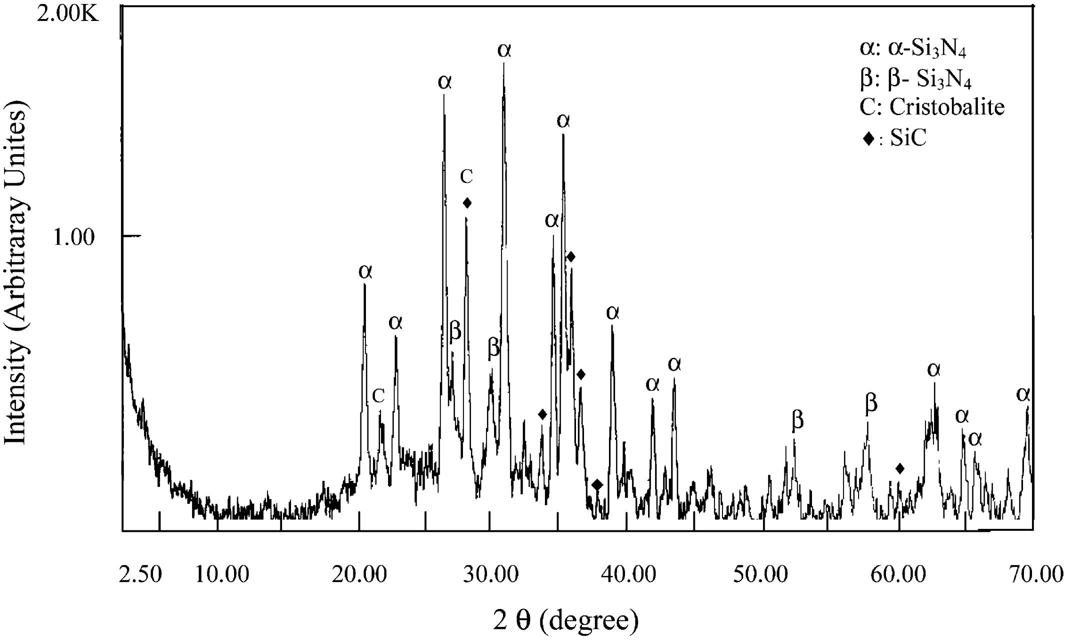

Fig. 10. XRD pattern of fibrous Si_3N_4 taken from top of the graphite boat (CTRN at 1400 °C for 4 h).

approximately 1–5 μm width and 5–10 μm in length (Fig. 12a and b). From the SEM analysis it was seen that a complete reduction and nitridation of SiO_2 took place on these products. The composition of resulting product was analyzed by EDAX, as indicated in Fig. 12c. After CTRN process the transformation product has only 2% wt. Al, and 1.99% wt. Fe as impurities. It is known that the K_2O, Na_2O, and MgO are largely lost at the carbo-thermal reduction stage.[25] SEM micrographs of product obtained at 1450 °C for 16 h CTRN process were similar to those of the product obtained at 1400 °C for 16 h CTRN process (Fig. 13).

3.2. Duration

Strongest Si_3N_4 peaks are belonging to 16 h CTRN processing, but at 1400, and 1450 °C major Si_3N_4 formation took place for 4, and 8 h processing. The overall

Table 3
Results of carbothermal reduction and nitridation of diatomite

CTRN duration (h)	CTRN temperature (°C)	Crystalline phases by XRD α/β[a]	Reaction weight loss (wt.%)[b]	Theoretical residual carbon (wt.%)[c]	Real residual carbon (wt.%)[d]
4	1350	30/70	15.9	29.1	34.9
8	1350	25/75	16.3	28.7	33.3
16	1350	20/80	16.6	28.4	33.1
4	1400	40/60	30.6	13.4	20.2
8	1400	30/70	33.3	11.7	17.6
16	1400	15/85	36.4	8.6	15.8
4	1450	35/65	30.8	14.2	19.5
8	1450	20/80	32.3	11.7	16.0
16	1450	10/90	35.6	9.4	16.8

[a] Calculated from XRD peak heights.
[b] Measured by weighting the original and the reacted samples.
[c] Calculated using the initial C content of samples.
[d] Measured by calcination in air at 800 °C for 2 h.

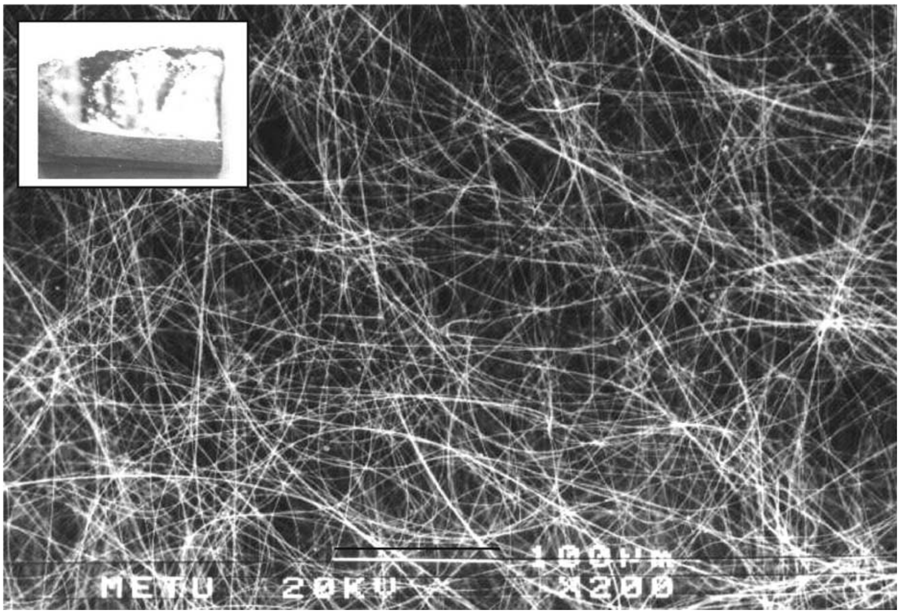

Fig. 11. SEM micrograph of α-Si_3N_4 fibers on the top of the carbon boat obtained at 1400 °C for 8 h.

stoichiometric equation for the carbothermal nitridation synthesis of Si_3N_4 is as follows reaction:[11]

$$3SiO_{2(s)} + 6C + 2N_{2(g)} \rightarrow Si_3N_{4(s)} + 6CO_{(g)} \quad (3)$$

This reaction is envisaged to proceed via a nucleation and growth process. First, SiO is formed at the contact points of C and SiO_2.

$$SiO_{2(s)} + C_{(s)} \rightarrow SiO_{(g)} + (CO)_{(g)} \quad (4)$$

Once CO is formed, SiO may form by the reduction of SiO_2 with CO

$$SiO_{2(s)} + CO_{(g)} \rightarrow SiO_{(g)} + CO_{2(g)} \quad (5)$$

$$C_{(s)} + CO_{2(g)} \rightarrow 2CO_{(g)} \quad (6)$$

The SiO reacts to form new Si_3N_4 nuclei in the following manner:

$$3SiO_{(g)} + 3C_{(s)} + 2N_{2(g)} \rightarrow Si_3N_{4(s)} + 3CO_{2(g)} \quad (7)$$

If the reaction occurs at a pre-existing nucleus, then a gas-phase growth reaction will occur over the graphite boats (Fig. 11).

$$3SiO_{(g)} + 3CO_{(g)} + 2N_{2(g)} \rightarrow \alpha\text{-}Si_3N_{4(s)} + 3CO_{2(g)} \quad (8)$$

For longer CTRN duration cotton-like products disappeared. It is believed that α-Si_3N_4 transformed into more stable β-Si_3N_4[22,23] and then major transformation took place in the boat direct to β-Si_3N_4 by the following reaction:

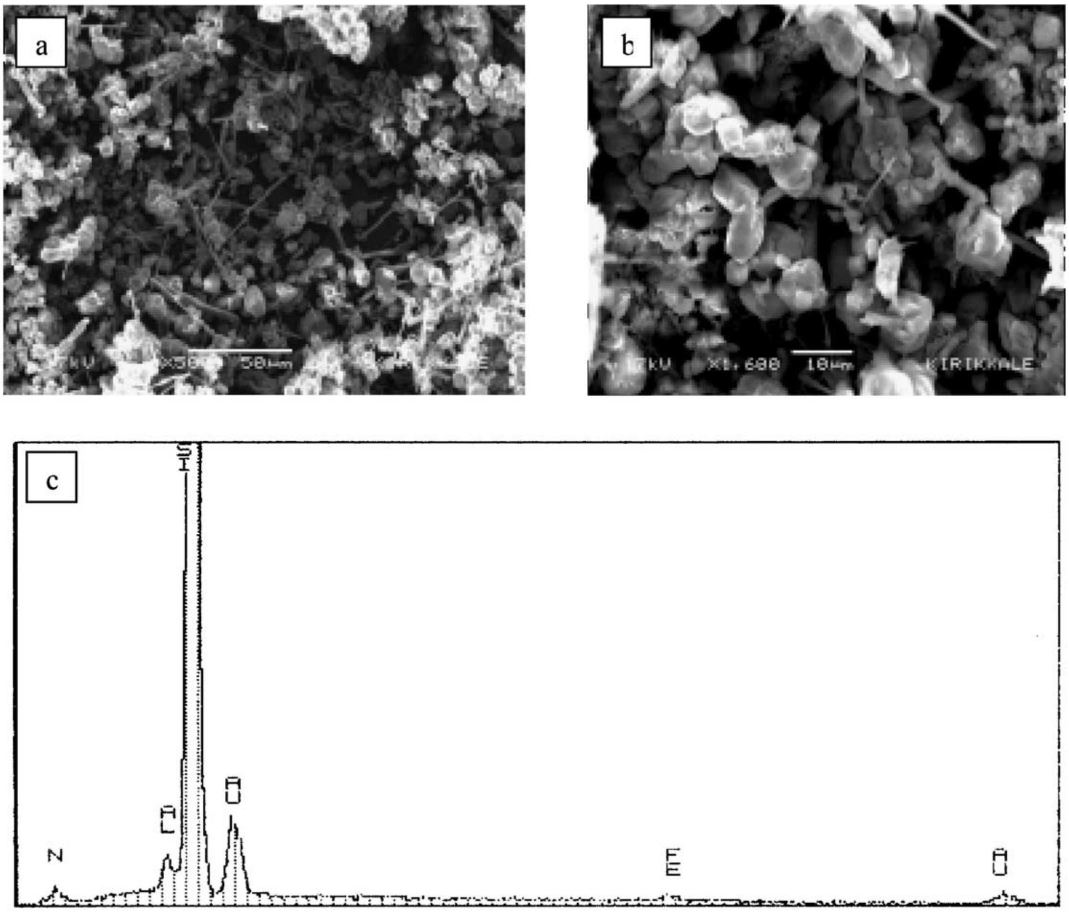

Element	K-ratio	Z	A	F	ZAF	Atom%	Wt %
Si-K	0.919	0.997	1.048	1.000	1.045	96.88	96.00
Al-K	0.019	1.021	1.082	0.936	1.034	2.11	2.00
Fe-K	0.017	1.162	1.021	1.000	1.186	1.01	1.99

Total: 100.00%

Fig. 12. SEM micrograph with EDAX analysis of CTRN product obtained at 1400 °C for 16 h: (a) general appearance of the transformation product in the graphite boat; (b) high magnification of globular morphology; (c) result of EDAX analysis taken from a single globular particle.

$$3SiO_{2(s)} + 6C + 2N_{2(g)} \rightarrow \beta\text{-}Si_3N_{4(s)} + 6CO_{(g)} \qquad (9)$$

In the literature,[19–21] higher temperatures but shorter duration are proposed for CTRN processing. Times up to 20 h have been reported but 6–8 h are recommended. In this work, removing of some impurities such as CaO, MgO, Na_2O_3, K_2O and complete transformation of diatomite to Si_3N_4 structure took place at 1400, and 1450 °C for 16 h CTRN treatments.

3.3. Products

XRD pattern of the sample that maximum transformation was observed, showed that all peaks were related to β-Si_3N_4. Under, normal conditions, α-Si_3N_4 was produced by CTRN process, but liquid phases of oxides such as K_2O, TiO_2, Fe_2O_3, and CaO contained in the diatomite occurred due to eutectic reaction, led to the formation of β-Si_3N_4 instead of α-Si_3N_4.[24] The intensity of peaks of α-Si_3N_4 on the XRD pattern of 4 h-processed product was gradually decreased with increase of CTRN duration. As a result, formation of β-Si_3N_4 instead of α-Si_3N_4 was controlled by oxides in diatomite and by the duration. SEM studies indicated that powder sample contained the particles of two different morphologies. Approximately 15% of the powder sample had fibrous structure with 0.5–3 μm in diameter and 10–40 μm in length (Fig. 12a), and rest of it consisted of hexagonal prisms with dimensions of 1–5 μm.

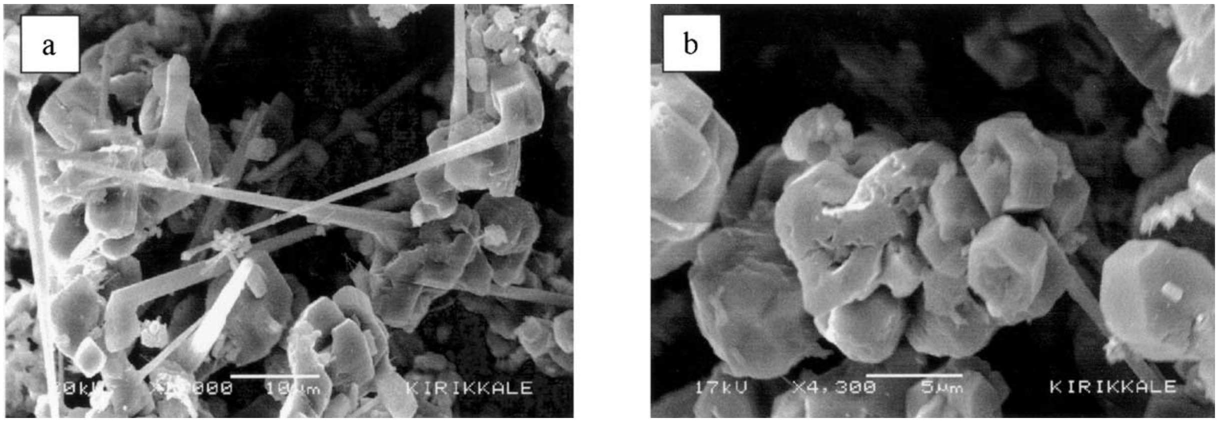

Fig. 13. SEM micrograph of CTRN product obtained at 1450 °C for 16 h: (a) globular and fiber structure; (b) globular morphology of β-Si_3N_4.

4. Conclusion

1. Si_3N_4 could be synthesized by CTRN process from diatomite. C/SiO_2 molar ratio of 4, temperature of 1400 °C and duration of 16 h are recommended.
2. Impurity oxides like Al_2O_3, K_2O, TiO_2, Fe_2O_3 and CaO promotes formation of β-Si_3N_4 instead of preferred α-Si_3N_4.
3. In the CTRN process, carbon reduces SiO_2 to pure silicon. Then pure silicon reacts with N_2 to form Si_3N_4.

References

1. Ziegler, G., Heinrich, J. and Wotting, G., *Mater. J. Sci.*, 1987, **22**, 3041.
2. Herrmann, M., Boberski, C., Michael, G., Putzky, G. and Hermel, W., *Mater. J. Sci. Let.*, 1993, **12**, 1641.
3. Jack, K. H., *Mater. J. Sci.*, 1976, **11**, 1135.
4. Jong, B. W., Slavens, G. J. and Traunt, D. E., *Mater. J. Sci.*, 1992, **27**, 6086.
5. Arik, H., Saritas, S. and Gunduz, M., *Mater. J. Sci.*, 1999, **34**, 835.
6. Kurt, A. O. and Davies, T. J., *Mater. J. Sci.*, 2001, **36**, 5895.
7. Arık, H. and Kadir, S., *Tr. J. Engin. Environ. Sci.*, 1999, **23**, 287.
8. Mazzonni, A. D. and Aglietti, E. F., *Applied Clay Sci.*, 1996, **11**, 143.
9. Mazzonni, A. D. and Aglietti, E. F., *Materials Chemistry and Physics*, 1997, **49**, 196.
10. Umebayashi, S. and Kobayashi, K., *J. Amer. Ceram. Soc.*, 1975, **58**, 9.
11. Weimer, A. W., Cassiday, J. R., Susnitzky, D. W., Black, C. K. and Beaman, D. R., *Mater. J. Sci.*, 1996, **31**, 6005.
12. Segal, D. L., *British Ceramic Transaction*, 1986, **85**, 184.
13. Sugahara, Y., Hiraiwa, H., Kuroda, K. and Kato, C., *Mater. J. Sci.*, 1988, **23**, 3181.
14. Hrabe, Z., Komarneni, S. and Malla, P., *Mater. J. Sci.*, 1992, **27**, 4614.
15. Valdes, J. J. P. and Rodriguez, A. V., *Mater. J. Sci. Let.*, 1992, **11**, 678.
16. Chang Zhang, S. and Roger Cannon, W., *Journal of the American Ceramic Society*, 1984, **67**, 691.
17. Kumar, B. and Godkhindi, M. M., *Mater. J. Sci. Let.*, 1996, **15**, 403.
18. Frederic, L., Kadey, J.R. *Industrial Minerals and Rocks*, Vol. 1, ed. J. S. Lefond et al. 1983, p. 677.
19. Aruntaş, H. Y., Albayrak, M. and Tokyay, H. A., *M. Tr. J. Engin. Environ. Sci.*, 1998, **22**, 337.
20. Arık, H., Kadir, S. and Aruntaş, H. Y., *J. Inst. Sci. Technol. Gazi University*, 2002, **15**, 103.
21. Perera, D. S., *Mater. J. Sci.*, 1987, **22**, 2411.
22. Sarın, V. K., *Mat. Sci. Engin.*, 1988, **A105/106**, 151.
23. Park, J. Y. and Kim, C. H., *J. Mater. Sci.*, 1988, **23**, 3049.
24. Peck, D. H., Kim, J. Y. and Choi, S. W., *Key Eng. Mater.*, 1994, **89–91**, 15.
25. Mostaghaci, H., Fan, Q. and Riley, F. L., *Br. Ceram. Trans. J.*, 1986, **85**, 12.